Journal of Materials and Environmental Science
ISSN : 2028-2508
e-ISSN : 2737-890X
CODEN : JMESCN

J. Mater. Environ. Sci., 2025, Volume 16, Issue 10, Page 1770-1787

http://www.jmaterenvironsci.com

Amino Acid Functionalized Eggshell for Divalent Iron Removal from Water: Insights into Equilibrium, Kinetics, Thermodynamics, and Antimicrobial Activity

Surya S. Nair [1], Devika Sathish [1], Pretty Ann Mathai [1], Anitha Jose [2], Shaji Varghese [1] *

[1]*PG and Research department of chemistry, Mar Thoma College, Tiruvalla, Pathanamthitta, Kerala 689103, India*

[2] *Department of Microbiology, Mar Thoma college, Tiruvalla, Pathanamthitta, Kerala 689103, Indi22*

**Corresponding author, Email address: shaji@mtct.ac.in*

Received *21 Aug 2025,*
Revised *12 Sept 2025,*
Accepted *14 Sept 2025*

Keywords:
- ✓ *Eggshell;*
- ✓ *L-cysteine functionalized eggshell;*
- ✓ *Iron adsorption;*
- ✓ *Kinetics;*
- ✓ *Antimicrobial;*
- ✓ *Escherichia coli;*

Citation*: Surya S Nair, Devika Sathish, Pretty Ann Mathai, Anitha Jose, Shaji Varghese (2025) Amino Acid Functionalized Eggshell for Divalent Iron Removal from Water: Insights into Equilibrium, Kinetics, Thermodynamics, and Antimicrobial Activity, J. Mater. Environ. Sci., 16(10), 1770-1787*

Abstract: We developed an L-cysteine functionalized adsorbent from bio-waste eggshells using the impregnation method. Characterization through Fourier Transform Infrared Spectroscopy (FTIR), X-ray diffraction (XRD), and Field Emission Scanning Electron Microscopy (FE-SEM) unveiled the presence of –NH and –C=O groups, a crystalline structure, and porous morphology. The effectiveness of the functionalized adsorbent for iron recovery from water was assessed under dynamic conditions, including pH, adsorbate concentrations, adsorbent dosages, temperature, and contact times. Notably, it gained a removal efficiency of 96.29% at a 20 mg/L iron concentration, with optimal conditions at pH 3, an adsorption capacity of 74.24 mg/g, a dosage of 50 mg, and a temperature of 306 K over 30 minutes. The adsorption process followed a pseudo-second-order model, while the equilibrium aligned with Freundlich isotherms. Thermodynamic parameters indicated that the removal of Fe (II) ions was exothermic and spontaneous. Additionally, the antimicrobial activity of the functionalized adsorbent (L-CFES) was tested against Gram-positive and Gram-negative bacteria, showing promising inhibition, particularly against Escherichia coli (23 mm zone of inhibition) compared to Staphylococcus aureus (20 mm). These outcomes reveal that the L-cysteine functionalized eggshell is a promising eco-friendly adsorbent for iron removal from water and has notable antibacterial properties.

1. Introduction

Water pollution by heavy metals is escalating due to rapid industrialization, urbanization, and the utilization of chemical substances in various industries (Qu et al., 2018**)**. The adverse effects of heavy metals, such as toxicity, non-biodegradability, biological accumulation, and carcinogenic nature, lead to global concern for the aquatic ecosystem and human health (Ahmadijokani *et al.*, 2022, Akessé *et al.*, 2022). The presence of these toxic heavy metals is detectable in streamlets and soils due to human activities (Vatanpour *et al.*, 2020). Surface water is connected to groundwater resources, the water cycle, the drinking water supply, and its significance in agriculture and aquatic

life, playing a crucial role in various fields such as the environment and human life (Alaba *et al.*, 2018). However, growing and exploring new and cost-effective strategies is essential to remove the alarming rate of heavy metal contamination from various environments (Hem, J. D. 1972; Razzouki *et al.*, 2015; Errich *et al.*, 2021; El Hammari *et al.*, 2022).

Iron is a naturally occurring heavy metal and a common contaminant in source water and wastewater. The mining and metallurgical industries are notable wastewater generators with high iron levels, releasing significant volumes into the environment. The damaging impact of iron on living organisms and infrastructure demands the development of efficient iron removal technologies for water treatments (Kaksonen & Janneck, 2024; Joseph & Haque, 2018). On the other hand, overexposure to iron can cause serious health diseases, including Hemochromatosis, cardiovascular disease, Diabetes mellitus, and neurological diseases (Wasserman *et al.*, 2006; Powers *et al.*, 2003; Kell, 2010).

Various physical, chemical, and biological methods are invented to remove heavy metals from wastewater, including adsorption, ion exchange, membrane technology, electrokinetic technology, chemical precipitation, photo remediation, biochar, etc. (Farina *et al.*, 2013; Hoang *et al.*, 2022; Karn *et al.*, 2021; Qasem *et al.*, 2021). The preference of methods depends on the nature of the heavy metal present, its concentration, and the wastewater characteristics to be taken for the treatment (Kumar *et al.*, 2022). Most of these techniques have limitations, such as pre-treatments and additional treatments for optimising effectiveness, and some of them are less effective and require high capital costs (Park *et al.*, 2005).

One of the versatile and practical approaches for removing heavy metals and contaminants from wastewater is adsorption (Patra *et al.*, 2020). Adsorption is a physicochemical technique with several advantages, such as operating at ambient temperature and removing multiple minerals simultaneously (Maleki *et al.*, 2015). Based on the availability, reusability, surface area, pore size, effectiveness in adsorbing metals, and cost-effectiveness, many materials can be used as adsorbents, including activated alumina, silica gel, activated carbon, ion-exchange resin, etc (Shahnaz *et al.*, 2020).

Egg shells are promising alternative bio adsorbents due to their natural porous structure, mechanical strength, thermal stability, and ability to remove heavy metals, dyes, pesticides, and contaminants from water and wastewater. Egg shells are readily available as by-products from various industries and households, making them low-cost and have attractive adsorption applications. Using eggshells can cause no pollution as they can be used as biowaste, offering environmental benefits (Ikram *et al.*, 2020).

Surface modification with various materials can enhance the adsorption properties of eggshells. Several research works show that the impregnation of salicylic acid onto the surface of calcinated eggshells improved their adsorption properties due to highly developed functionalized surface area and rich pore properties (Tsai *et al.*, 2006). On the other hand, various metal oxides and metal oxo hydroxide functionalized eggshells can also enhance adsorption capacity, and metal ion-modified eggshells are highly effective because they are cost-effective and environmentally generous (Almeida *et al.*, 2020, Bayode *et al.*, 2024).

In this work, we developed an amino acid L-Cysteine functionalized eggshell (L-CFES) sample for iron adsorption from water. L-cysteine acts as an activating agent that influences the activated eggshell's surface area and pore size. This work explores the adsorptive performance of L-CFES, which is eco-friendly for removing iron from water and includes the adsorption kinetics and

equilibrium. This study examines adsorption phenomena, specifically equilibrium and kinetics, using Langmuir and Freundlich isotherms and pseudo-first-order and pseudo-second-order kinetics. Studies on various parameters such as pH, contact time, adsorbate concentration, and adsorbent dosage help to explore their influence on adsorption. This work manifests its potential for iron removal from contaminated water.

2. Methodology

2.1 . Materials

All chemical reagents utilized in this study were of analytical grade, highly purified, and used without additional purification. The experiments were carried out using double distilled water, hydrochloric acid, sodium hydroxide, L-cysteine (AR grade), and ferrous sulphate heptahydrate (AR grade) sourced from Avra Synthesis Private Limited (India). The chicken eggshells were obtained from the college canteen.

2.2 Extraction of eggshell powder (ES)

The eggshells collected were meticulously washed with double distilled water to eliminate impurities. Subsequently, the membrane mass of the eggshell was removed by treating 10% hydrochloric acid solution for one hour. Following this step, they were rewashed with double distilled water and left to dry at room temperature. Once dried, the eggshells were finely powdered using a mortar and pestle. The resulting powdered eggshells were then utilized for subsequent modifications.

2.3 Preparation of L-Cysteine Functionalized Eggshell (L-CFES) adsorbent

About 0.0605 g of L-Cysteine was dissolved in 50 mL of double distilled water, and then 1 g of finely powdered eggshell was added to the solution. After stirring the resulting mixture for 4 hours at room temperature, the solution was filtered, and the residue was dried at 80°C in a hot air oven. The dried powder was then transferred into a vacuum container as an adsorbent.

2.4 Characterization of adsorbent

The ES and L-CFES FTIR spectra were recorded at room temperature with a Shimadzu spectrophotometer in the IR region of 4000- 400 cm^{-1} with a resolution of 4 cm^{-1} and 32 scans per second. The X-ray powder diffraction (XRD) can be conducted by using a PANalytical Aeris Research diffractometer with CuKα X-ray source to determine the crystallographic structure of the powdered material. Electron microscopic analysis was obtained by using MAIA3 XMH FESEM with EDX.

2.5. Microbial strains

The in vitro antibacterial effects of eggshell, L-cysteine, and L-cysteine functionalized eggshell adsorbents were tested against Gram-positive and Gram-negative bacterial strains, including Staphylococcus aureus and E-coli. Bacterial strains were cultured in a Nutrient agar medium.

2.6 Antimicrobial screening

The antimicrobial assay was carried out in Muller Hinton Agar plates. The test organisms (E. coli and Staphylococcus aureus) were inoculated in nutrient broth and incubated overnight at 37 º C. MHA plates were prepared and inoculated with test organisms (E coli and S. aureus) from nutrient broth. Sterile discs were placed on the surface of the inoculated MHA plate, and 20 µL of sample L-CFES

and eggshell was added to the sterile disc. Sterile water served as the negative control. All the plates were then incubated at 37º C for 24 to 48 hours. Following incubation, the diameter of the inhibition zone was measured in millimeters.

2.7. Batch adsorption experiments

The adsorption studies experiments were evaluated using batch adsorption. About 50 mg of the adsorbent was diffused in a 50 mL solution containing 20 mg/L of divalent Fe (II). The aqueous solution was mechanically shaken for about 30 minutes. The percentage adsorption of the material is measured at different time intervals (0,10, 15, 20, 25, and 30 minutes) using a Shimadzu UV-visible spectroscope. The adsorption capacity of the adsorbent was obtained using **Eqn.** $qe = (C_0 - C_e) \times \frac{V}{m}$ *Equ.1* as:

$$qe = (C_0 - C_e) \times \frac{V}{m} \quad \text{Equ.1}$$

Eqn. 2 explains the obtained removal efficiency $\% \, removal = \frac{C_0 - C_e}{Ce} \times 100$ *Eqn. 2*

$$\% \, removal = \frac{C_0 - C_e}{Ce} \times 100 \quad \text{Eqn. 2}$$

Where q_e represents the adsorption capacity of functionalized eggshell per gm of adsorbent, C_0 (mg/L) is the initial concentration of Fe (II) solution, C_e (mg/L) is the equilibrium concentration of the Fe (II) solution, m is the mass of the adsorbent in grams, V is the volume of the adsorbate solution in litre.

The influences of the experimental parameters such as pH, adsorbent dosage (10-50mg), and metal ion concentration (20-200 mg/L) were also investigated.

3. Adsorption equilibrium

3.1. Adsorption isotherms

To analyse the nature of the adsorption process, equilibrium adsorption isotherms were studied to understand how an adsorbate interacts with the adsorbent. Three types of the well-known two-parameter adsorption isotherm models, namely Langmuir (**Eqn.** $\frac{1}{q_e} = \frac{1}{K_L q_m}\frac{1}{C_e} + \frac{1}{q_m}$ Eqn.3) and Freundlich (**Eqn.** $logq_e = logK_F + \frac{1}{n} logC_e$ Eqn.4), were fitted to analyse the adsorption equilibrium data. The following equations describe the Langmuir and Freundlich isotherms ($\frac{1}{q_e} = \frac{1}{K_L q_m}\frac{1}{C_e} + \frac{1}{q_m}$ Eqn.3- $logq_e = logK_F + \frac{1}{n} logC_e$ Eqn.4) respectively (Varghese *et al.*, 2024). The R_L value corresponding to the Langmuir isotherm can also be determined according to **Eqn.** $R_L = \frac{1}{1+K_L C_0}$ Eqn.5.

$$\frac{1}{q_e} = \frac{1}{K_L q_m}\frac{1}{C_e} + \frac{1}{q_m} \quad \text{Eqn.3}$$

$$logq_e = logK_F + \frac{1}{n} logC_e \quad \text{Eqn.4}$$

$$R_L = \frac{1}{1+K_L C_0}$$ Eqn.5

Ce (mg/L) is the equilibrium ion concentration, q_e (mg/g) is the amount of ions adsorbed at equilibrium, q_m (mg/g) is the number of ions required to form a monolayer, K_L(L/mg) is the Langmuir isotherm constant related to the energy of adsorption, K_F (mg/g) is. The Freundlich constant is related to adsorption capacity, and 1/n is the empirical parameter that denotes adsorption intensity.

3.2. Kinetic studies

Adsorption kinetic studies provide valuable insights into the adsorption mechanism and reaction pathway. Utilising kinetic models such as the pseudo-first order and pseudo-second order, we can assess the effectiveness of the process. The pseudo-first-order and pseudo-second-order models are employed to evaluate the rate of the adsorption process (Varghese *et al.*, 2024). The equations can be given as:

Pseudo-first order kinetic equation : $ln\,(q_e - q_t) = lnq_e - K_1 t$ Eqn.6

Pseudo-second order kinetic equation: $\frac{t}{q_t} = \frac{1}{K_2 q_e^2} + \frac{t}{q_e}$ Eqn.7

3.3. Thermodynamic studies

The values of ΔH^0 and ΔS^0 for the adsorption process were determined from the slope and intercept of the graph plotted between ln K and 1/T. Thermodynamic parameters, including Gibbs free energy (ΔG^0), enthalpy (ΔH^0), and entropy (ΔS^0), are employed to assess the feasibility and spontaneity of the adsorption process at different temperatures. These parameters can be calculated as follows:

$$\Delta G = RTlogK_L$$ Eqn.8

$$logK_L = -\frac{\Delta H}{RT} + \frac{\Delta S}{R}$$ Eqn.9

Where R is the universal gas constant (8.314 J/mol/K), T (K) is the adsorption temperature, and K_L is the adsorption equilibrium constant (q_e/C_e). The values of ΔH and ΔS for the adsorption process is determined from the slope and intercept of the graph plotted between log K_L and 1/T.

4. Results and Discussion

4.1. Characterization

4.1.1. SEM/EDX Analysis

SEM was used to determine the surface characteristics of the L-cysteine functionalized eggshell (L-CFES). Previous studies show eggshells (ES) have a homogeneous and porous surface (Daraei *et al.*, 2013). **Figure 1(a)** shows the surface morphology of the L-CFES; the shape and size of the adsorbents are flake, rod-like, irregular, and sparsely distributed, and the porous nature of the surface is also manifest. These pores play an essential role in iron adsorption into the L-CFES adsorbent. The EDX spectra and elemental mapping of L-CFES are shown in **Figure 1 (b) and (c).** The surface elemental composition of the material is found to be Ca, Mg, C, O, N, and S. The obtained results support the previous finding reported in (Isa *et al.*, 2020, Rahmani-Sani *et al.*, 2020). This is also confirmed by the FT-IR and XRD analysis of L-CFES, which is reported in **Figure 2** and **Figure 3.**

4.1.2. XRD Analysis

Figure 2 shows the X-ray diffraction patterns of ES and L-CFES***Figure 2***. The samples exhibit characteristic diffraction peaks with diffraction angles at 23.2^0, 29.4^0, 31.9^0, 36.1^0, 42.8^0, 47.7^0, 48.9^0, 57.3^0, 64.6^0, and 66.2^0. The high intense peak marked at 29.5^0 (2θ) conveys that both the eggshell powder and L- cysteine functionalized eggshell contains a thermodynamically stable calcite crystalline structure, which is identical to calcium carbonate ($CaCO_3$) (Onwubu *et al.*, 2017). In addition to this, additional peaks at diffraction angles 18.9^0, 28.5^0, 33.03^0, and 34.8^0 are observed in L-CFES, depicting the monoclinic crystal structure of L-cysteine (NR and I SL, 2016). This result also confirms the presence of amino acids on the surface of the eggshell powder.

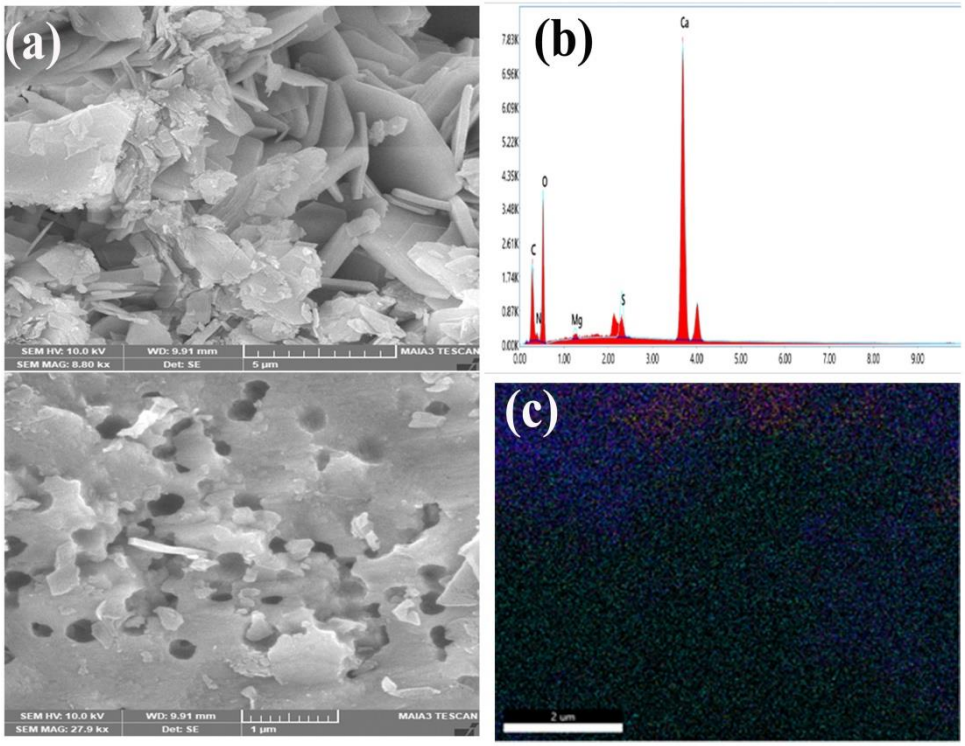

Figure 1: (a) SEM images of L-CFES, (b) EDX data, (c) Elemental mapping of L-CFFES

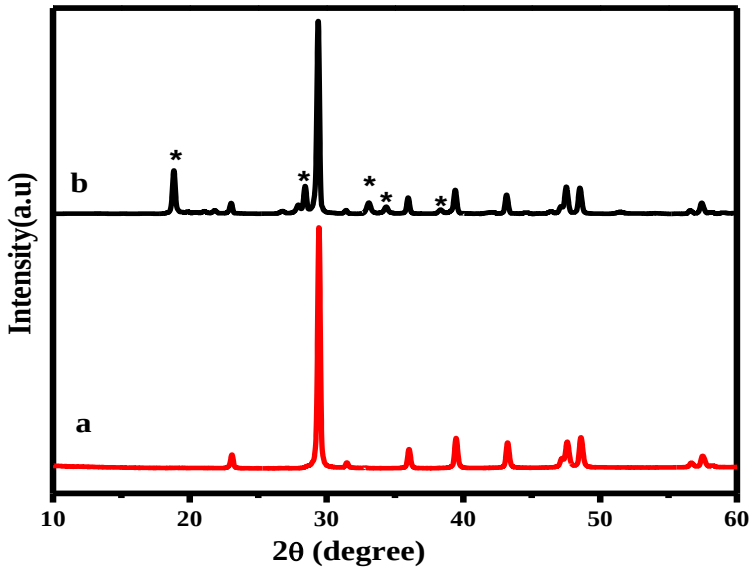

Figure 2: XRD pattern of (a) ES and (b) L-CFES

4.1.3. FT-IR Analysis

Characterization of L-cysteine functionalized eggshell (L-CFES) was accomplished by FT-IR spectroscopy. **Figure 3** illustrates the FT-IR spectrum of the (a) eggshell, (b) L-cysteine and (c) L-cysteine functionalized eggshell. The eggshell and L-cysteine functionalized eggshell show distinct peaks at 711 cm^{-1}, 873 cm^{-1}, 2521 cm^{-1} and 3313 cm^{-1}, respectively. An intense peak was observed at 1413 cm^{-1} in ES and L-CFES, attributed to carbonate minerals within the eggshell matrix. The broadband observed at 3600-3000 cm^{-1} is attributed to the presence of hydroxyl groups on the surface of the eggshell. In the L-cysteine FT-IR spectrum, an absorption peak is observed at 2143 cm^{-1} due to -N-H stretching vibration and additional peaks are present at 1593 cm^{-1} and 1494 cm^{-1} due to symmetric and asymmetric –C-O-O stretching vibration (Laskar *et al.*, 2018). The FT-IR spectra of L-CFES show similarity to the spectrum of L-cysteine, indicating the presence of similar functional groups on the surface of the eggshell.

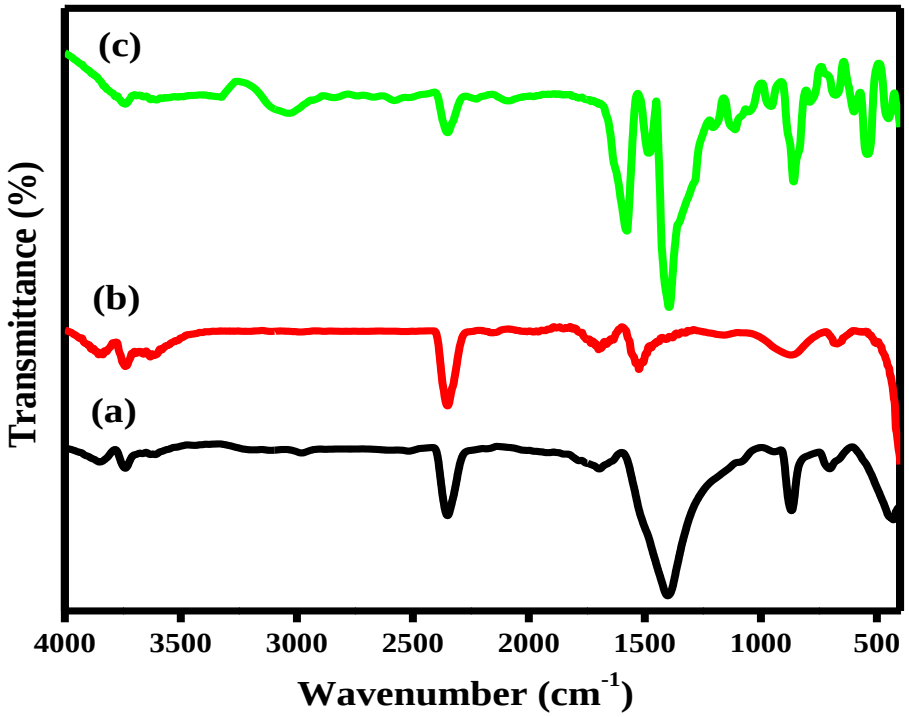

Figure 3: FT-IR spectra of **(a)** ES, **(b)** L-cysteine, and **(c)** L-CFES

4.2. Adsorption Studies

4.2. 1. Effect of Contact time

The experimental result on the effect of contact time on iron adsorption is shown in **Figure 4** (a). The rate of adsorbate removal was rapid for the first 10 minutes at pH 5, and this trend continued until the 25-minute mark, at which point the 30-minute mark reached equilibrium. This behavior is attributed to gradually occupying initially available vacant sites over time. At equilibrium, there is a reduction in the number of active sites available, leading to a decrease in the driving force for adsorption and, consequently, minimal or no further adsorption. As time progresses, the quantity of accessible sites decreases, causing congestion of the adsorbent within the pores, thereby impeding the movement of the adsorbate (Varghese *et al.*, 2024).

4.2.2. Effect of Adsorbent dosage

Figure 5 shows the impact of adsorbent dosage on the efficiency of iron adsorption. It highlights the key finding that the optimal adsorption capacity of 96.29% is achieved with a 50mg dosage of L-CFES. Both texts emphasise that beyond this optimal dosage, the adsorption efficiency declines due to the saturation of surface sites, leading to decreased iron removal efficiency. The adverse effects of higher adsorbent doses, such as particle aggregation, congestion, and overlapping, which lead to reduced surface area and sorption capacity, are consistently noted. This demonstrates a clear understanding of how varying the dosage of L-CFES affects the adsorption process, supporting the conclusion that there is an optimal adsorbent dosage for maximising iron removal efficiency (Abatan *et al.*, 2020).

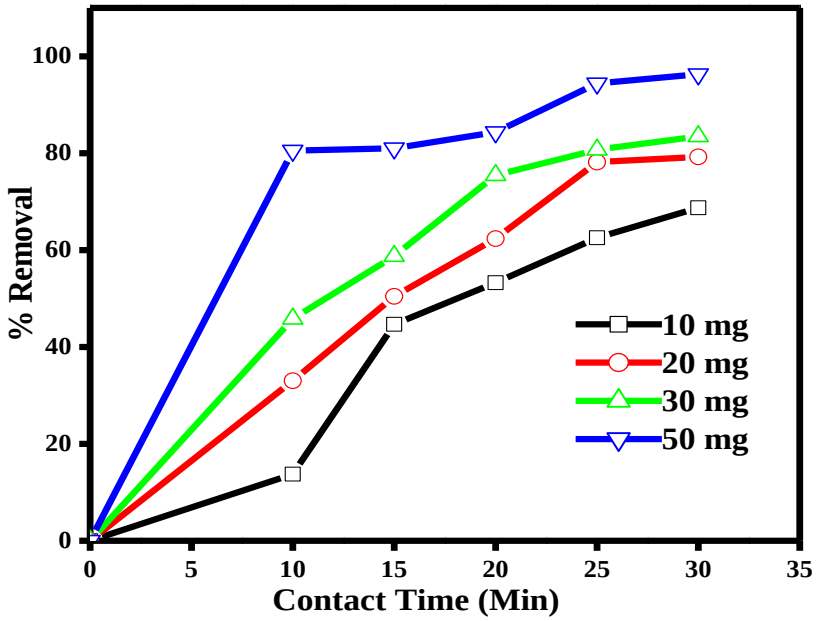

Figure 4: Effect of contact time with % removal of Fe(II) solution

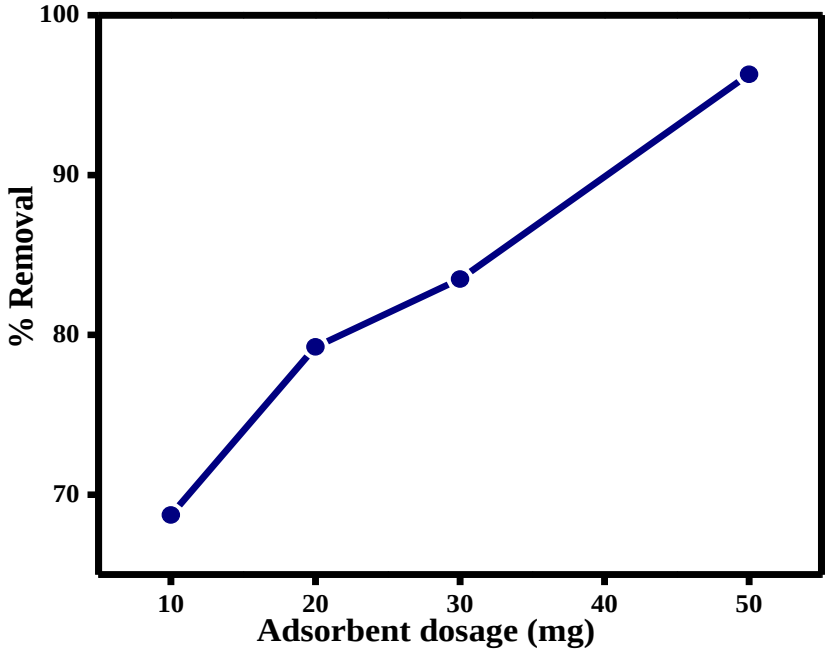

Figure 5: Effect of different dosages of L-CFES with % removal of Fe (II)solution

4.2.3. Effect of initial concentration of Iron (II) solution

The influence of Fe (II) concentration was examined by varying the concentration of adsorbate from 20, 50, 100,150 and 200 mg/L while keeping the adsorbent dosage constant at 50mg a, the contact time at 30 min, and the optimum pH at 3. **FFigure 6** shows that the initial concentration of iron solution affects the adsorption efficiency of L-CFES. However, as depicted in **Figure 6**, there is a decrease in the adsorption percentage of L-CFES material with an increase in adsorbate concentration from 50 to 200 mg/L. At a concentration of 20 mg/L, the adsorption percentage is higher, attributed to the large availability of surface sites on the adsorbent for adsorption at lower adsorbate concentrations. Lower initial concentrations of the Fe (II) solution allow more solute to be adsorbed until equilibrium.

Consequently, the surface sites of the adsorbent gradually become saturated, leading to a progressive decrease in the adsorption rate of the adsorbent. Compared to 50, 100, 150 and 200 mg/L concentrations, the higher adsorption rate observed at 20 mg/L (96.29%) of iron can be attributed to increased adsorption efficiency. This trend is likely due to the pores in the adsorbent becoming clogged as the concentration of metal increases (Abatan *et al.*, 2020).

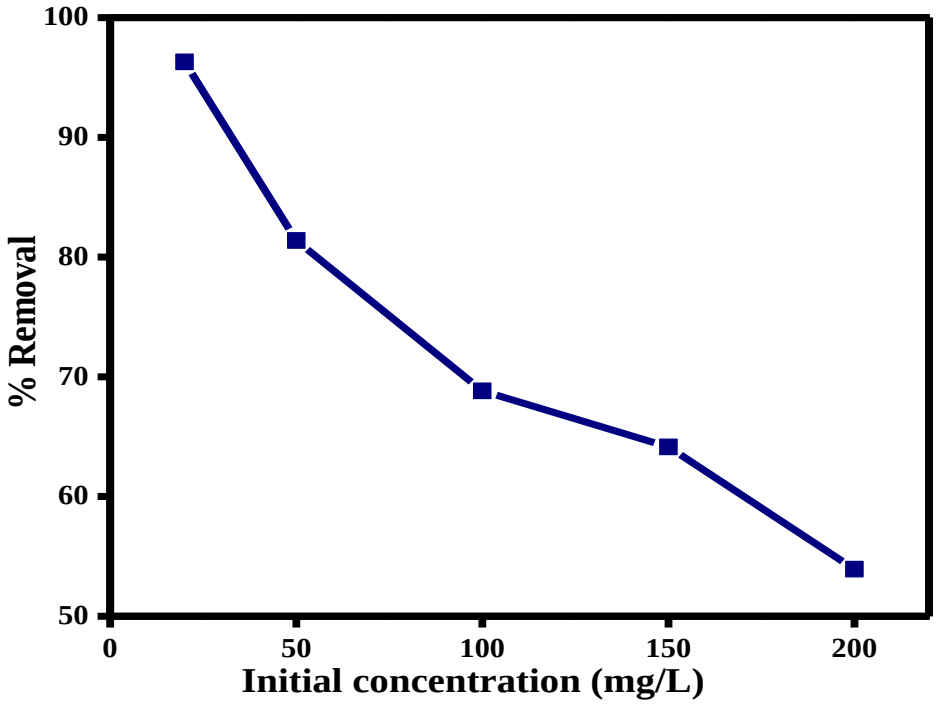

Figure 6: Effect of initial concentration of Fe (II) solution versus % removal of Fe (II) ion

4.2.4. Effect of pH

The pH value of a solution plays a crucial role in the adsorption process. The Iron adsorption onto amino acid functionalized eggshell surfaces at different pH levels studied ranged from 3 to 11. From **Figure 7**, we can find that pH 3 shows the highest adsorption, which suggests that the functionalization of eggshell surfaces with amino acid plays a significant role in enhancing iron adsorption under acidic conditions. This could be due to various factors, such as the protonation of functional groups on the amino acids, which may increase the affinity of the surface for iron ions. The decrease in iron adsorption with increasing pH could be attributed to changes in the speciation of the functional groups within the amino acids and the adsorbent surface. Certain functional groups may deprotonate at higher pH levels, altering their ability to interact with iron ions effectively.

Understanding the speciation of functional groups and the surface chemistry at different pH levels is crucial for optimising adsorption processes (NR and I SL, 2016).

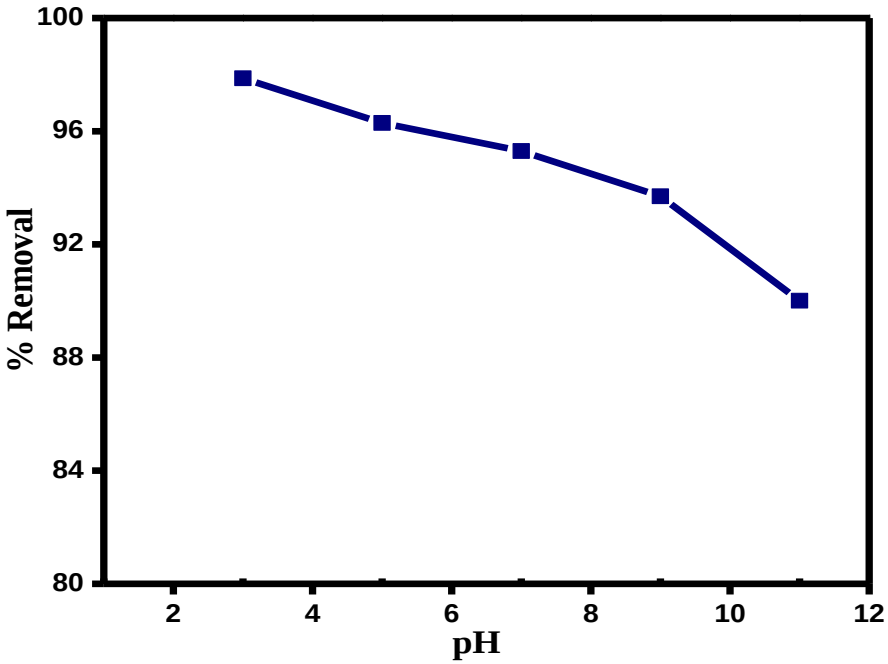

Figure 7: Effect of pH on % removal of Fe (II) over L-CFES

4.2.5. Effect of Temperature

Temperature is a critical factor for adsorption processes. The principles of thermodynamics play a significant role in the relation between adsorbent and adsorbate molecules. When the adsorption capacity of the adsorbent increases with temperature, it suggests an endothermic adsorption process, whereas a decrease in adsorption capacity with temperature indicates an exothermic adsorption process. The effect of temperature on the adsorption of iron solution onto the adsorbent was studied at 326, 336, 346 and 356 K. In **Figure 8**, the experimental results show a decrease in the removal percentage of iron as the temperature increases from 326 K to 356 K.

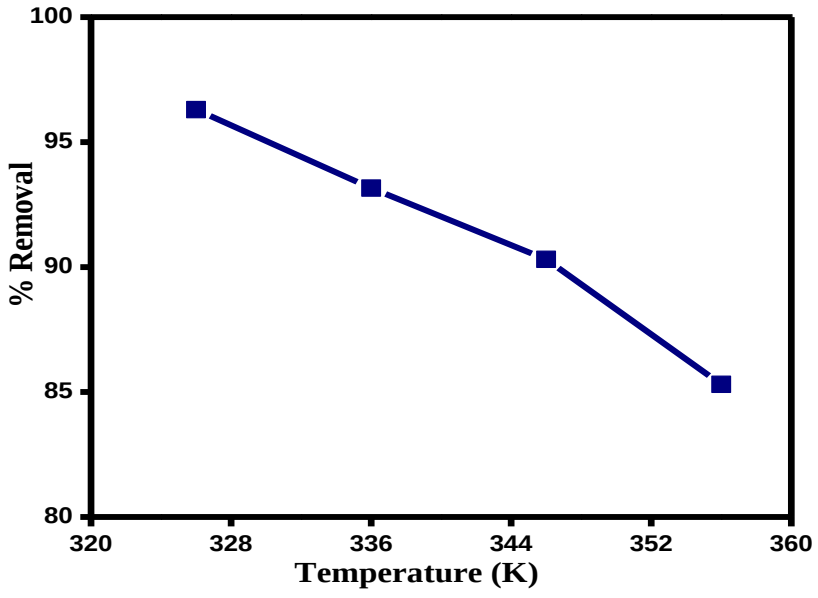

Figure 8: Effect of Temperature on % removal of Fe (II) over L-CFES

This observation suggests that the adsorption process for iron onto the adsorbent is likely exothermic. In exothermic adsorption processes, a temperature rise typically diminishes the adsorption capacity. This phenomenon occurs because the additional thermal energy interferes with the adhesive forces between the adsorbent and adsorbate molecules. Consequently, fewer adsorbate molecules are effectively maintained on the adsorbent surface (Adebayo *et al.*, 2016).

4.3. Adsorption isotherm

Adsorption isotherm models are crucial for optimizing the adsorbent and explaining the relationship between the adsorbate molecules and the adsorbent, thereby determining the adsorption capacities of the adsorbent molecules (Varghese *et al.*, 2024). **Figure 9** represents the adsorption equilibrium isotherms associated with iron adsorption onto the functionalized eggshell using (a) Langmuir and (b) Freundlich models.

Table 1: Isotherm constants and regression coefficient values for the adsorption of Fe(II) by L-CFES

Adsorption isotherms	Isotherm parameters	Regression coefficients R^2
Langmuir model	q_m (mg g^{-1}) = 74.2391 K_L (L mg^{-1}) = 0.4665 R_L = 0.6345	0.9242
Freundlich model	K_F = 3.7002 n =2.7604 1/n = 0.3623	0.9892

The isotherm constants and equation parameters associated with the isotherms are listed below in **Table 1**. The high R^2 value of the Freundlich adsorption model indicates a strong fit for adsorption studies. This explains the adsorption process as reversible and non-ideal, forming the non-uniform multilayers of the iron metal on the L-CFES surface. Moreover, the nature of the adsorption of Iron by L-CFES was obtained by the equilibrium parameter (R_L). The adsorption is more satisfactory when R_L is between 0 and 1. **TTable 1** reveals that the R_L values for the adsorption of metal ions by L-CFES are favorable. The adsorption capacity of the functionalized eggshell is 74.2391 mg/g for iron, as shown in **Table 1**. This result indicates that L-CFES exhibited prominently greater adsorption capacities than unmodified eggshell (Yeddou and Bensmaili, 2007). For the Freundlich adsorption isotherm model, the value of exponent n has a magnitude of 2.9501, showing that the process favors physical adsorption. The 1/n value for the Freundlich adsorption model is <1, which shows a less cooperative adsorption process, and the heterogenous efficiency increases that will be more at low adsorbate concentrations (Varghese *et al.*, 2024).

4.4. Adsorption Kinetics

Adsorption kinetics pertains to the speed at which a substance is either retained or released from a liquid solution at the interface of a solid. The analysis of adsorption can be carried out using linear or non-linear methods. Studies on adsorption kinetics offer valuable insights into the quality of the adsorbent, its efficacy in removing substances, the rate of the adsorption process, the attainment of equilibrium, and the fundamental mechanism of adsorption (Magdy *et al.*, 2018). The kinetic model mathematically describes how metal particles move from the bulk solution to the biosorbent surface.

The study utilized the pseudo-first-order and pseudo-second-order kinetic models (Holliday *et al.*, 2024). The rate constants, adsorption capacities and correlation coefficients for the pseudo-first order and pseudo-second order adsorption of iron at different concentrations by L-CFES are displayed in **Error! Reference source not found.**.

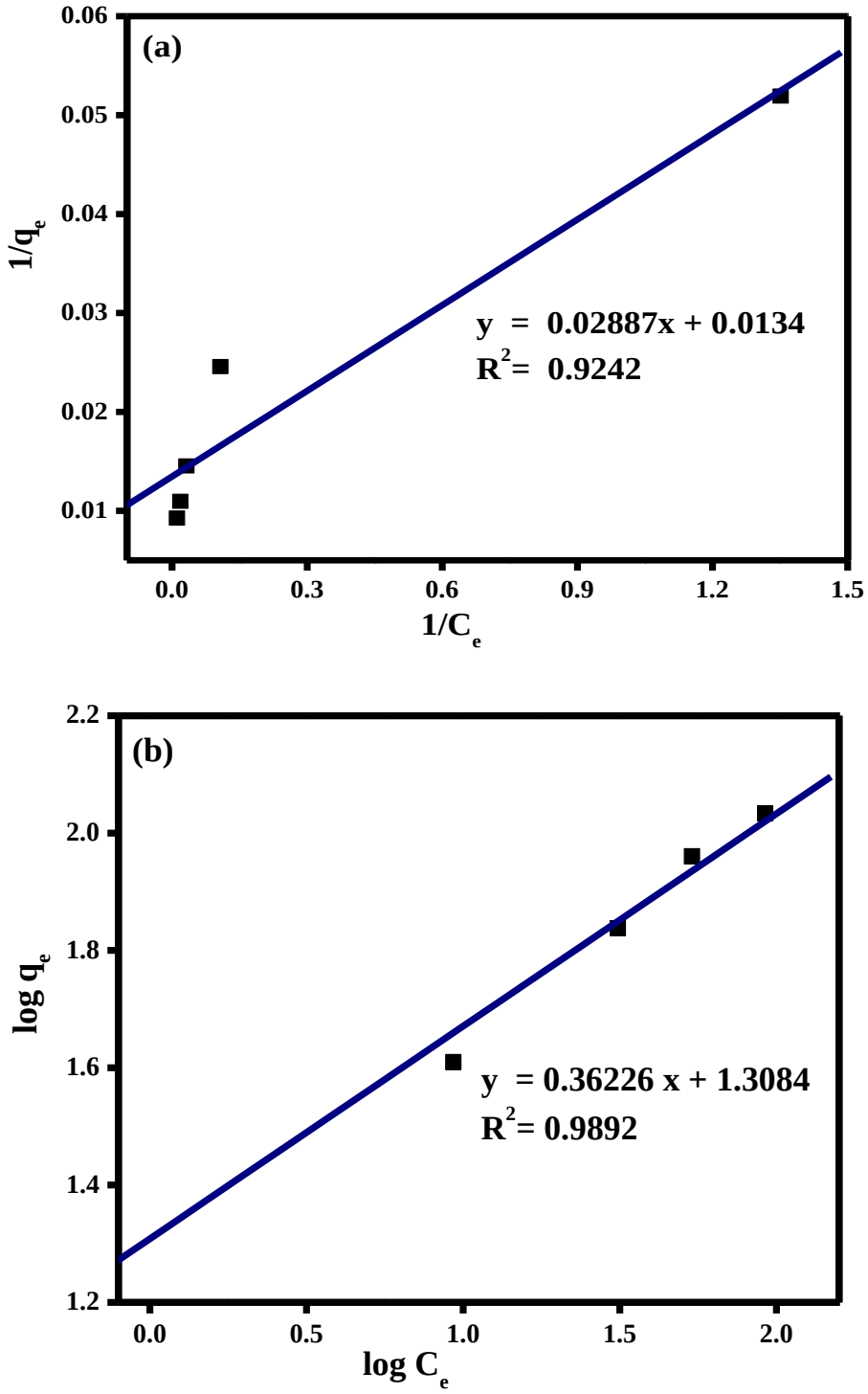

Figure 9: Isotherm model for Fe (II) adsorption (a) Langmuir and (b) Freundlich by L-CFES

The experimental data for iron adsorption kinetics onto L-cysteine functionalized eggshells were analysed using pseudo-first and pseudo-second-order models. The experimental results in **Error! Reference source not found.** indicate that the data does not fit well with the pseudo-first-order model, as evidenced by the low R^2 values. In contrast, the pseudo-second-order model better fits

higher R^2 values. This suggests that metal adsorption onto L-CFES follows pseudo-second-order kinetics, reflecting a chemical interaction between the iron molecules and the functional groups on the adsorbent's surface, critical to its adsorption capacity (Varghese *et al.*, 2024). The calculated and experimental values of q_e are closer to the second-order kinetic model than the first-order kinetic model at all concentrations, suggesting that the Fe (II) adsorption process by L-CFES shows a better correlation to the second order kinetic model.

Table 2: Rate constants and regression data for Fe (II) adsorption by L-CFES

Iron C_0 (mg/L)	q_e Calculated (mg/g)	Pseudo-first-order kinetics			Pseudo second-order kinetics		
		K_1 (min^{-1})	q_e (mg/g)	R^2	K_2 (mg/g/min)	q_e (mg/g)	R^2
20	19.26	0.013891	773.426	0.60426	0.026850802	20.22245	0.99824
50	40.69	0.011309	472.0666	0.653	0.010842483	43.2526	0.99938
100	68.822	0.015019	2649.96	0.58778	0.01202222	71.02273	0.9995
150	96.21	0.011092	496.7714	0.68006	0.009961412	99.20635	0.99992
200	108	0.006952	79.29301	0.79502	0.00655947	238.0952	0.9996

4.5. Thermodynamic Studies

The properties such as spontaneity and feasibility of adsorption processes can be understood by determining the thermodynamic parameters like standard Gibbs free energy(ΔG^0), enthalpy (ΔH^0) and entropy (ΔS^0). Calculation of the thermodynamic parameters Enthalpy (ΔH^0), Entropy(ΔS^0), and Gibbs free energy (ΔG^0) of adsorption on L-CFES are shown in **Table 3.**

Iron adsorption on the L-CFES material shows a negative standard Gibbs free energy value to be spontaneous and thermodynamically favored at all the studied temperatures. The value of $\Delta G°$ in between the range -4 to -8 KJ/mol suggests the process to be physisorption. The adsorption of heavy metals on L-CFES shows the negative value of $\Delta G°$ increases as the temperature increased from 306 K – 336 K, indicating that adsorption was more favourable at lower T, nearly room temperature. Weak van der Waals forces hold the adsorbate molecules onto the adsorbent surface at lower temperatures. The rise in temperature causes the adsorbate molecules to gain kinetic energy, which leads to the desorption of adsorbate molecules, resulting in decreases in the favourability of adsorption. The negative value for the standard enthalpy changes obtained shows that the adsorption process is exothermic. The magnitude of $\Delta H°$ describes whether the process is physisorption or chemisorption. The value of ΔH^0 in between the range 40-400 KJ/Mol indicates the process to be highly exothermic and, therefore, tends to physisorption due to chemical reactions. Furthermore, the negative $\Delta S°$ entropy change suggests decreased disorder or randomness during adsorption. The confinement of adsorbate molecules to the adsorbent surface limits the freedom of movement of molecules and their possible orientations, resulting in a decrease in entropy, which indicates the process to be physisorption (Sharma *et al.*, 2022, Thommes *et al.*, 2015).

Table 3: Thermodynamic parameters for the adsorption of Fe (II) solution by L-CFES

Temperature (K)	K_L	ΔG^0 (KJ/Mol)	ΔH^0 (KJ/Mol)	ΔS^0 (J/K/Mol)
306	26.02	-8.29		
316	13.62	-6.86		
326	9.31	-6.04	-41.787	-109.845
336	5.80	-4.91		

4.6. Antimicrobial Assay

Antimicrobial activity of the L-CFES and eggshell powder were analysed for two bacteria, Gram-positive Staphylococcus aureus and Gram-negative E-coli. The obtained result is reported in **Figure 10**. The highest activity of the functionalised adsorbent was found against E-coli with an inhibition zone of 23 mm compared to gram-positive bacteria, for which Staphylococcus aureus showed an inhibition zone of 20 mm. The controlled sample used was sterile distilled water, which shows no inhibition zone. The eggshell powder alone shows no antimicrobial activity against the selected bacteria strains. The superior activity of L-CFES is due to the active surface functional groups present in the eggshell material.

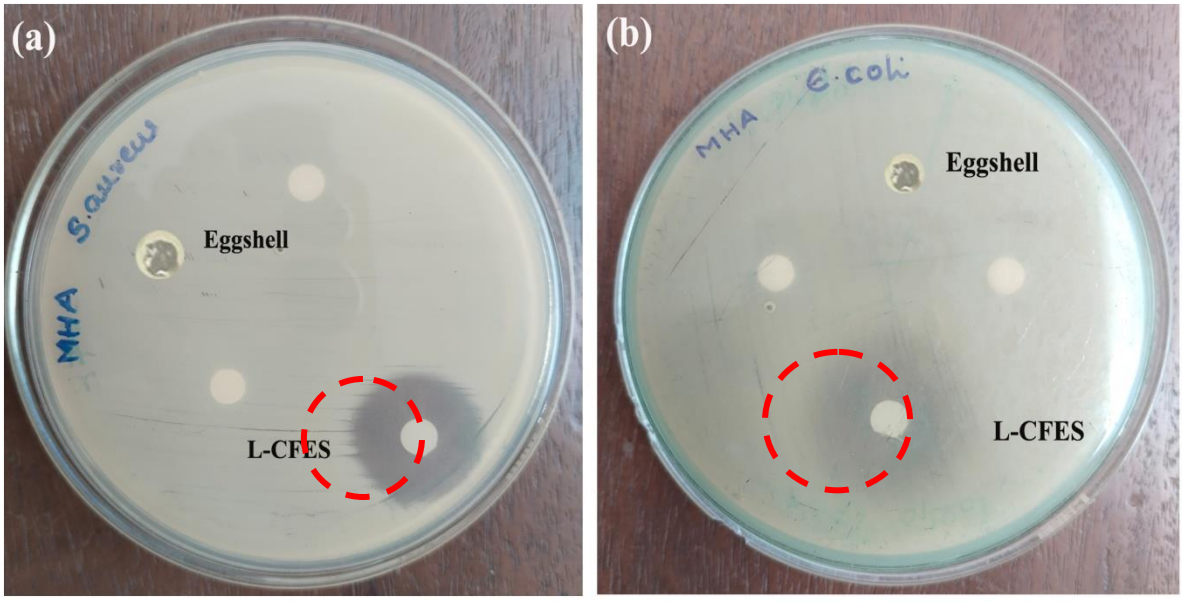

Figure 10: Antimicrobial activity of L-CFES; (a) Gram-positive Staphylococcus aureus and (b) Gram-negative E-coli

5. Conclusion

This study prepared L-CFES from waste eggshells to recover metals like Fe from water. The prepared adsorbent was characterised using FTIR, XRD and FE- SEM with EDS spectra. The removal efficiency of the adsorbent was carried out using various parameters such as solution pH, adsorbate concentration, adsorbent dosage, contact time and temperature. The optimum conditions for the results show that the maximum adsorption capacity of the adsorbent was 74.2391 mg/g at an

initial concentration of 20mg/L, the adsorbent dosage of 50 mg, pH of 3 and temperature of 306 K for 30 minutes. The best adsorption was attained at pH 3, indicating that the L-CFES exhibited adsorption performance at acidic conditions. The equilibrium observations revealed that the Freundlich model is a better match for the adsorption of Fe (II). Considering the value of R^2 and variance between the predicted and experimental values of q_e, the best model for removing Fe (II) from water is pseudo-second-order kinetics. Fe (II) adsorption was exothermic and spontaneous from a thermodynamic outlook. The antimicrobial activity of the L-CFES showed superior activity against Gram-positive Staphylococcus aureus and Gram-negative E. coli compared to bare eggshells. Based on the results, it can be concluded that L-CFES can be utilised as a favourable and resilient adsorbent to recover Fe (II) from water. It is also helpful for the antimicrobial treatment of water bodies.

Acknowledgement: The authors thank the Department of Microbiology, Mar Thoma College, Tiruvalla, Kerala, for the antimicrobial analysis. The authors acknowledge DST-FIST, Mar Thoma College, Tiruvalla, for FT-IR and UV-visible analysis and also thank SAIF, Mahatma Gandhi University, for FESEM- EDX instrumental facilities.

Disclosure statement: *Conflict of Interest:* The authors declare that there are no conflicts of interest.
Compliance with Ethical Standards: This article does not contain any studies involving human or animal subjects.

References

Abatan, O. G.; Alaba, P. A.; Oni, B. A.; Akpojevwe, K.; Efeovbokhan, V.; Abnisa, F. Performance of Eggshells Powder as an Adsorbent for Adsorption of Hexavalent Chromium and Cadmium from Wastewater. *SN Appl. Sci.* 2020, *2*, 1996. DOI: 10.1007/s42452-020-03866-w.

Abid, B. A.; Brboot, M. I.; Al-Shuwaiki, N. M. Removal of Heavy Metals Using Chemicals Precipitation. *Eng. Technol. J.* 2011, *29*, 595–612. DOI: 10.30684/etj.29.3.15.

Adebayo, G. B.; Mohammed, A. A.; Sokoya, S. O. Biosorption of Fe(II) and Cd(II) Ions from Aqueous Solution Using a Low Cost Adsorbent from Orange Peels. *J. Appl. Sci. Environ. Manage.* 2016, *20*, 702–714. DOI: 10.4314/jasem.v20i3.25.

Ahmadijokani, F.; Molavi, H.; Peyghambari, A.; Shojaei, A.; Rezakazemi, M.; Aminabhavi, T. M.; et al. Efficient Removal of Heavy Metal Ions from Aqueous Media by Unmodified and Modified Nanodiamonds. *J. Environ. Manage.* 2022, *316*, 115214. DOI: 10.1016/j.jenvman.2022.115214.

Akessé D. P. V., Dalogo K. A. P., Kouadio D. L., C. Koffi A. L., Mamadou K. (2022). Assessment of metal pollution (Fe, Cu, Cd, Pb, Hg) of an aquatic mining environment: case of the BOZI gold panning area (Marahoué region), *J. Mater. Environ. Sci.*, 13(9), 1067-1080

Alaba, P., Oladoja, N., Sani, Y. M., Ayodele, O., Mohammed, I., Olupinla, S., *et al.* (2018). Insight into Wastewater Decontamination Using Polymeric Adsorbents. *J. Environ. Chem. Eng. 6*, 1651–1672. DOI: 10.1016/j.jece.2018.02.019.

Almeida, P. V.; Santos, A. F.; Lopes, D. V.; Gando-Ferreira, L. M.; Quina, M. J. (2020). Novel Adsorbents Based on Eggshell Functionalized with Iron Oxyhydroxide for Phosphorus Removal from Liquid Effluents. *J. Water Process Eng. 36*, 101248. DOI: 10.1016/j.jwpe.2020.101248.

Bahar Laskar, I.; Rajkumari, K.; Gupta, R.; Chatterjee, S.; Paul, B.; Lalthazuala Rokhum, S. (2018). Waste Snail Shell Derived Heterogeneous Catalyst for Biodiesel Production by the Transesterification of Soybean Oil. *RSC Adv. 8*, 20131–20142. DOI: 10.1039/C8RA02397B.

Bayode, A. A.; Badamasi, H.; Olusola, J. A.; Durodola, S. S.; Akeremale, O. K.; Ore, O. T.; et al. One-Pot Synthesis of ZnO-Activated Eggshell@kaolinite: Sorbents for Phosphate Capture in Water. *Chem. Eng. Technol.* 2024, *47*, 375–386. DOI: 10.1002/ceat.202300176.

Daraei, H.; Mittal, A.; Noorisepehr, M.; Daraei, F. Kinetic and Equilibrium Studies of Adsorptive Removal of Phenol onto Eggshell Waste. *Environ. Sci. Pollut. Res.* 2013, *20*, 4603–4611. DOI: 10.1007/s11356-012-1409-8.

El Hammari L., Latifi S., Saoiabi S., Saoiabi A., Azzaoui K., *et al.* (2022), Toxic heavy metals removal from river water using a porous phospho-calcic hydroxyapatite, *Mor. J. Chem.* 10(1), 62-72, https://doi.org/10.48317/IMIST.PRSM/morjchem-v10i1.31752

Errich A., Azzaoui K., Mejdoubi E., Hammouti B., Abidi N., Akartasse N., Benidire L., EL Hajjaji S., Sabbahi R., Lamhamdi A. (2021), Toxic heavy metals removal using a hydroxyapatite and hydroxyethyl cellulose modified with a new Gum Arabic, *Indonesian Journal of Science & Technology*, 6(1), 41-64

Farina, M.; Avila, D. S.; da Rocha, J. B. T.; Aschner, M. Metals, Oxidative Stress and Neurodegeneration: A Focus on Iron, Manganese and Mercury. *Neurochem. Int.* 2013, *62*, 575–594. DOI: 10.1016/j.neuint.2012.12.006.

Hem, J. D. Chemical Factors That Influence the Availability of Iron and Manganese in Aqueous Systems. In *Geological Society of America Special Papers, Vol. 140*; Geological Society of America, 1972; pp 17–24. DOI: 10.1130/SPE140-p17.

Hoang A.T., Nižetić S., Cheng C.K., Luque R., Thomas S., Banh T.L., et al. Heavy Metal Removal by Biomass-Derived Carbon Nanotubes as a Greener Environmental Remediation: A Comprehensive Review. *Chemosphere* 2022, *287*, 131959. DOI: 10.1016/j.chemosphere.2021.131959.

Holliday, M. C.; Parsons, D. R.; Zein, S. H. Agricultural Pea Waste as a Low-Cost Pollutant Biosorbent for Methylene Blue Removal: Adsorption Kinetics, Isotherm and Thermodynamic Studies. *Biomass Convers. Biorefin.* 2024, *14*, 6671–6685. DOI: 10.1007/s13399-022-02865-8.

Ikram, M.; Raza, A.; Imran, M.; Ul-Hamid, A.; Shahbaz, A.; Ali, S. Hydrothermal Synthesis of Silver Decorated Reduced Graphene Oxide (rGO) Nanoflakes with Effective Photocatalytic Activity for Wastewater Treatment. *Nanoscale Res. Lett.* 2020, *15*, 95. DOI: 10.1186/s11671-020-03323-y.

Isa, Y. M.; Harripersadth, C.; Musonge, P.; Sayago, A.; Morales, M. G. The Application of Eggshells and Sugarcane Bagasse as Potential Biomaterials in the Removal of Heavy Metals from Aqueous Solutions. *S. Afr. J. Chem. Eng.* 2020, *34*, 142–150. DOI: 10.1016/j.sajce.2020.08.002.

Joseph, G.; Haque, S. *Promising Progress. A Diagnostic of Water Supply, Sanitation, Hygiene, and Poverty in Bangladesh.* 2018. DOI: 10.13140/RG.2.2.30301.87527.

Kaksonen, A. H.; Janneck, E. (2024) Biological Iron Removal and Recovery from Water and Wastewater. In *Microbial Metal and Metalloid Metabolism*; Springer, Berlin, Heidelberg, n.d.; pp 1–58. DOI: 10.1007/10_2024_255.

Karn, R.; Ojha, N.; Abbas, S.; Bhugra, S. A Review on Heavy Metal Contamination at Mining Sites and Remedial Techniques. *IOP Conf. Ser.: Earth Environ. Sci.* 2021, *796*, 012013. DOI: 10.1088/1755-1315/796/1/012013.

Kell, D. B. Towards a Unifying, Systems Biology Understanding of Large-Scale Cellular Death and Destruction Caused by Poorly Liganded Iron: Parkinson's, Huntington's, Alzheimer's, Prions, Bactericides, Chemical Toxicology and Others as Examples. *Arch. Toxicol.* 2010, *84*, 825–889. DOI: 10.1007/s00204-010-0577-x.

Kumar, V.; Shah, M. P.; Shahi, S. K. Phytoremediation Technology for the Removal of Heavy Metals and Other Contaminants from Soil and Water. Elsevier, 2022. https://doi.org/10.1016/C2020-0-02583-1

Magdy, Y. M.; Altaher, H.; ElQada, E. Removal of Three Nitrophenols from Aqueous Solutions by Adsorption onto Char Ash: Equilibrium and Kinetic Modeling. *Appl. Water Sci.* 2018, *8*, 26. DOI: 10.1007/s13201-018-0666-1.

Maleki, A.; Hayati, B.; Naghizadeh, M.; Joo, S. W. Adsorption of Hexavalent Chromium by Metal Organic Frameworks from Aqueous Solution. *J. Ind. Eng. Chem.* 2015, *28*, 211–216. DOI: 10.1016/j.jiec.2015.02.016.

NR, I SL. Synthesis of L-Cysteine Capped ZnSe QDs and Their Photocatalytic Activity. *IJEAS* 2016, *3*, 257654. ISSN: 2394-3661

Onwubu, S. C.; Vahed, A.; Singh, S.; Kanny, K. M. Physicochemical Characterization of a Dental Eggshell Powder Abrasive Material. *J. Appl. Biomater. Funct. Mater.* 2017, *15*, e341–e346. DOI: 10.5301/jabfm.5000361.

Park, H.-J.; Bong, S.-H.; Jeong, S.-U. Removal of Heavy Metals(Pb, Cr) Using Waste Eggshell. In *Proceedings of the Korean Environmental Health Society Conference*, 2005; pp 386–393.

Patra, C.; Shahnaz, T.; Subbiah, S.; Narayanasamy, S. Comparative Assessment of Raw and Acid-Activated Preparations of Novel *Pongamia pinnata* Shells for Adsorption of Hexavalent Chromium from Simulated Wastewater. *Environ. Sci. Pollut. Res. Int.* 2020, *27*, 14836–14851. DOI: 10.1007/s11356-020-07979-y.

Powers, K. M.; Smith-Weller, T.; Franklin, G. M.; Longstreth, W. T.; Swanson, P. D.; Checkoway, H. Parkinson's Disease Risks Associated with Dietary Iron, Manganese, and Other Nutrient Intakes. *Neurology* 2003, *60*, 1761–1766. DOI: 10.1212/01.wnl.0000068021.13945.7f.

Qasem, N. A. A.; Mohammed, R. H.; Lawal, D. U. Removal of Heavy Metal Ions from Wastewater: A Comprehensive and Critical Review. *Npj Clean Water* 2021, *4*, 1–15. DOI: 10.1038/s41545-021-00127-0.

Qu, L.; Huang, H.; Xia, F.; Liu, Y.; Dahlgren, R. A.; Zhang, M.; et al. Risk Analysis of Heavy Metal Concentration in Surface Waters Across the Rural–Urban Interface of the Wen-Rui Tang River, China. *Environmental Pollution* 2018, *237*, 639–649. DOI: 10.1016/j.envpol.2018.02.020.

Rahmani-Sani, A., Singh, P., Raizada, P., Lima, E. C., Anastopoulos, I., Giannakoudakis, D. A., et al. Use of Chicken Feather and Eggshell to Synthesize a Novel Magnetized Activated Carbon for Sorption of Heavy Metal Ions. *Bioresour. Technol.* 2020, *297*, 122452. DOI: 10.1016/j.biortech.2019.122452.

Razzouki B., El Hajjaji S., Azzaoui K., Errich A., Lamhamdi A., Berrabah M., Elansari L.L. (2015). Physicochemical study of arsenic removal using iron hydroxide, *J. Mater. Environ. Sci.* 6 (5) (2015) 1444-1450

Shahnaz, T.; Patra, C.; Sharma, V.; Selvaraju, N. A Comparative Study of Raw, Acid-Modified and EDTA-Complexed *Acacia auriculiformis* Biomass for the Removal of Hexavalent Chromium. *Chem. Ecol.* 2020, *36*, 360–381. DOI: 10.1080/02757540.2020.1723560.

Sharma, T.; Chaturvedi, K. R.; Trivedi, J. *Nanotechnology for CO2 Utilization in Oilfield Applications*; Gulf Professional Publishing, 2022. https://doi.org/10.1016/C2020-0-03629-7

Thommes, M.; Kaneko, K.; Neimark, A. V.; Olivier, J. P.; Rodriguez-Reinoso, F.; Rouquerol, J.; et al. Physisorption of Gases, with Special Reference to the Evaluation of Surface Area and Pore Size Distribution (IUPAC Technical Report). *Pure Appl. Chem.* 2015, *87*, 1051–1069. DOI: 10.1515/pac-2014-1117.

Tsai, W. T.; Yang, J. M.; Lai, C. W.; Cheng, Y. H.; Lin, C. C.; Yeh, C. W. Characterization and Adsorption Properties of Eggshells and Eggshell Membrane. *Bioresour. Technol.* 2006, *97*, 488–493. DOI: 10.1016/j.biortech.2005.02.050.

Varghese, A. G.; Sathish, D.; Haritha, L. P.; Pillai, S. S.; Paul, S. A.; Latha, M. S. Fabrication of Citric-Acid-Modified Cellulose Adsorbent for Remediation of Methylene Blue Dye from Aqueous Solutions: Equilibrium, Kinetic, and Thermodynamic Studies. *Fibers Polym.* 2024, *25*, 3343–3355. DOI: 10.1007/s12221-024-00647-9.

Vatanpour, N.; Feizy, J.; Hedayati Talouki, H.; Es'haghi, Z.; Scesi, L.; Malvandi, A. M. The High Levels of Heavy Metal Accumulation in Cultivated Rice from the Tajan River Basin: Health and Ecological Risk Assessment. *Chemosphere* 2020, *245*, 125639. DOI: 10.1016/j.chemosphere.2019.125639.

Wasserman, G. A.; Liu, X.; Parvez, F.; Ahsan, H.; Levy, D.; Factor-Litvak, P.; et al. Water Manganese Exposure and Children's Intellectual Function in Araihazar, Bangladesh. *Environ. Health Perspect.* 2006, *114*, 124–129. DOI: 10.1289/ehp.8030.

Yeddou, N.; Bensmaili, A. Equilibrium and Kinetic Modelling of Iron Adsorption by Eggshells in a Batch System: Effect of Temperature. *Desalination* 2007, *206*, 127–134. DOI: 10.1016/j.desal.2006.04.052.